# Left Ventricular Regional Shape Dynamics Analysis by Three-dimensional Cardiac Magnetic Resonance Imaging Associated with Left Ventricular Function in First-time Myocardial Infarction Patients

Min Wan[1], Teo Soo Kng[1], Xulei Yang[1], Jun-Mei Zhang[2], Xiaodan Zhao[2], Wong Sum Thai[1], Calvin Lim Chi Wan[1], Liang Zhong[2,3], Ru San Tan[2,3], and Yi Su[1]

***Abstract*— Geometric remodelling of the left ventricle (LV) following myocardial infarction reflects on the geometric characteristics directly. This study focuses on a potential index based on curvedness. Nine consecutive normal volunteers and thirty consecutive myocardial infarction patients underwent MRI scan (twenty-seven patients had follow-up scan). Short-axis cine images of all cases were delineated. Three dimensional LV models were reconstructed and restored for possible motion distortion. The curvedness values were computed over 16-segments nomenclature. The curvedness signal for each segment over twenty-two time frames were fitted using a second order Fourier Series. Fourier coefficients were extracted and unsupervised learning was conducted between normal and patient data. An accuracy of $89\%$ and adjusted Rand Index of $0.5374$ suggest that these Fourier Series and curvedness based features can be an useful index for prognosis and diagnosis in clinical practice.**

## I. INTRODUCTION

Myocardial Infarction (MI) is an ischemic heart disease of the myocardial tissue, which is usually accompanied by left ventricular (LV) remodeling and loss of contractility [1], [2], [3], [4]. The geometry of the LV is complicated, and a comprehensive three dimensional approach to evaluate the ventricular contractility and geometric dynamics throughout the cardiac cycle is needed. Magnetic resonance imaging (MRI) is a superior approach to quantitatively assess the structure and function [5], [6], in comparison to echocardiography [7], ventriculography [8], [9], angiography [10] and indicator-dilution methods [11].

Even though the significance of geometric characteristics in the analysis of ventricular anatomies and functions has been recognized for decades, much of the earlier works had been either of a qualitative nature, or based on an ideal geometric prototype [12], [13], [4], [14] . The demand of a patient-specific quantitative geometry approach motivates this study.

[1]M Wan, S-K Teo, X Yang, C-W Lim, S-T Wong, Y Su are with Institute of High Performance Computing, Fusionopolis, 1 Fusionopolis Way, Singapore 138632 {wanm,teosk,yangx,limcw,wongst,suy} at ihpc.a-star.edu.sg

[2]J-M Zhang, X Zhao, L Zhong, R-S Tan are with National Heart Centre Singapore, 17 Third Hospital Avenue, Mistri Wing, Singapore 168752 {zhang.junmei,zhao.xiaodan} at nhcs.com.sg

[3]L Zhong, R-S Tan are with Duke-NUS Medical Graduate School, 169857, Singapore. {zhong.liang,tan.ru.san} at nhcs.com.sg, {zhong.liang,tan.ru.san}at duke-nus.edu.sg

The present study investigates the potential relation between the geometric dynamics and the clinician standard based on a three-dimensional approach. Patient-specific three-dimensional models were reconstructed from magnetic resonance images. The surface shape descriptor, i.e., curvedness, was computed over the obtained model. Curvedness values were averaged on the 16-segment LV nomenclature proposed by the American Heart Association (the apical segment in the 17-segment model was not considered in our study). The above computation was performed for each time frame. For each segment on the LV model, a curvedness-time signal was obtained. A second-order Fourier Series function was utilized to fit this time signal. The corresponding Fourier coefficients from all 16 fitted functions were extracted as the feature indicating the LV geometric dynamics. Such features were acquired from both volunteers and MI patients, and were used in an unsupervised learning, i.e., clustering. Only the cluster number was assigned in the learning procedure. The clustering results were evaluated using various criteria, including accuracy, unadjusted/adjusted Rand Index, and false positive/negative.

The remainder of this article is organized as follows. Section 2 describes the methodology. Section 3 provides the experimental results and the evaluation from several criteria. Section 4 concludes this article.

## II. METHODS

Short-axis MR images were processed in the CMRtools suite (Cardiovascular Solution, UK). Endocardium was delineated by experts for each slice. The stack of two dimensional contours were projected into three dimensional space. LV geometric shapes were then reconstructed via an in-house software for all temporal phases [15], [16].

The 3D geometric meshes generated were post-processed using geometric smoothing and restoration [17]. The principal curvatures at each mesh vertices were computed using a quadric surface fitting algorithm. So was the curvedness, which has been validated as a useful geometric descriptor in ventricular function assessment [15], [18].

According to the guideline of the American Heart Association, the sixteen regions (excluding the apical one) of the LV were extracted and the per-vertex curvedness value over each region was averaged. On each region, a time series

978-1-4244-7929-0/14/$26.00 ©2014 IEEE 

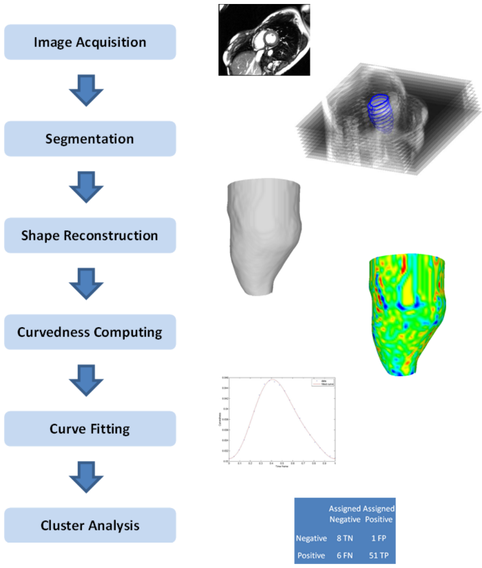


Fig. 1. Flow-chart of our method

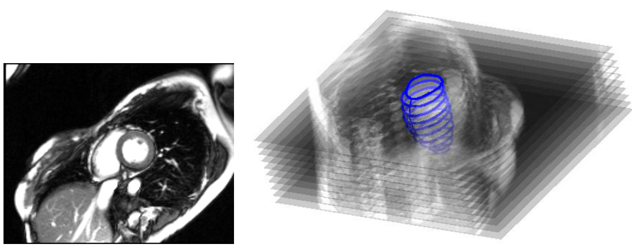

(a) Short axis MR image (b) Contours in 3D space

Fig. 2. MR images and contours

representing the varying curvedness over cardiac phases was obtained. Second order Fourier series were used to fit the time series to eliminate the high frequency component, i.e., noises. To explore the differences of curvedness time series patterns between normals and MI patients, cluster analysis was performed on all cases using Fourier series coefficients.

The whole procedure of our study is illustrated by the flow-chart in Figure 1. Each step is explained in detail in following subsections.

### A. Curvature and Curvedness Computing

LV geometric models were reconstructed from segmented endocardium contours via an in-house software, see the contours in Figure 2. The reconstructed LV models were represented by triangulated surface meshes. To evaluate the curvature at a vertex on the mesh, a local quadric surface geometry was fitted to the region [19], [20], [21], [22], [23]. The normal curvature was then computed as follows.

$$\kappa(\lambda) = \frac{L + 2M\lambda + N\lambda^2}{E + 2F\lambda + G\lambda^2}\,, \tag{1}$$

where $\lambda = \frac{dv}{du}$ such that $u$ and $v$ are the parameters of the underlying geometry, and $\{E, F, G\}$ and $\{L, M, N\}$ are components of the first and second fundamental forms,

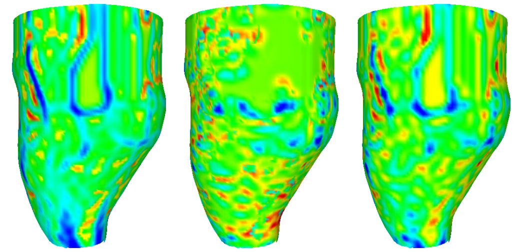

(a) $\kappa_1$ (b) $\kappa_2$ (c) $C$

Fig. 3. Principal curvatures and curvedness

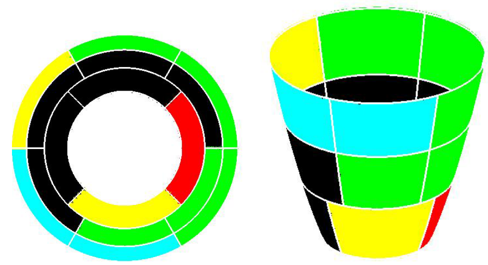

(a) Curvedness on bulleye view (b) Curvedness on 3D view

Fig. 4. Curvedness on 16 regions

repectively. Principal curvatures are defined as the extreme values of $\kappa(\lambda)$, $\kappa_1$, $\kappa_2$, which are the roots of the following equation.

$$\begin{bmatrix} L - \kappa E & M - \kappa F \\ M - \kappa F & N - \kappa G \end{bmatrix} = 0 \tag{2}$$

Koenderink [24] defined a shape descriptor curvedness value ($C$) as follows.

$$C = \sqrt{\frac{\kappa_1^2 + \kappa_2^2}{2}} \tag{3}$$

Curvedness has been proven to be a useful index for evaluating ventricular anatomy and function in our previous studies [9], [25], [21], see the illustration of curvature and curvedness on a LV model in Figure 3.

### B. Curve Fitting via Fourier Series

According to the guideline of the American Heart Association, the LV could be segmented into 17 regions. Excluding the apical region, we computed an average curvedness value for all 16 regions, see Figure 4. Hence for each region, a time series consisting of curvedness value throughout the cardiac cycle was obtained $C_{Seg}(t), 1 \leq Seg \leq 16, t = t_1, t_2, \cdots, t_{22}$.

A Fourier Series function was used to fit the curvedness-time signal. An $n$-order Fourier Series function is as follows with parameters $\{\mathbf{a}, \mathbf{b}, \omega\}$ :

$$f(\mathbf{a}, \mathbf{b}, \omega, t) = a_0 + \sum_{i=1}^{n} a_i \cos(i\omega t) + b_i \sin(i\omega t) \tag{4}$$

where $\mathbf{a} = [a_0, a_1, \cdots, a_n]'$ and $\mathbf{b} = [b_1, \cdots, b_n]'$.

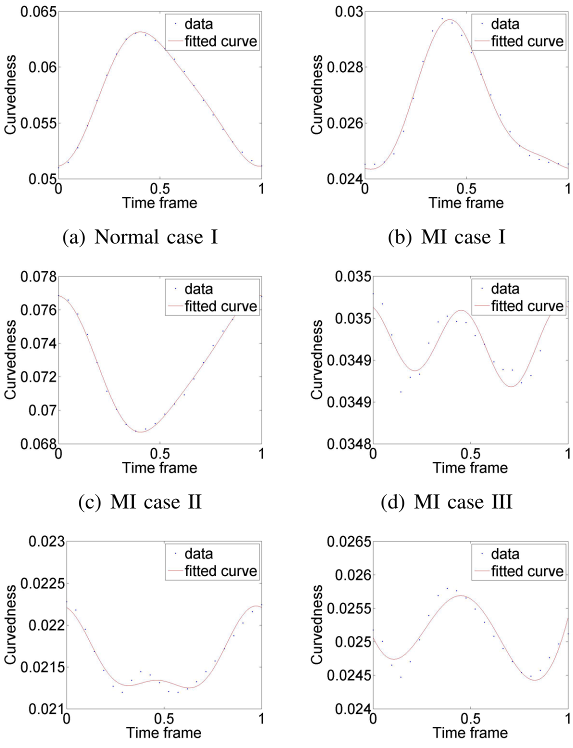


(a) Normal case I (b) MI case I (c) MI case II (d) MI case III (e) MI case IV (f) MI case V

Fig. 5. Examples of curvedness signals for normal and MI patients

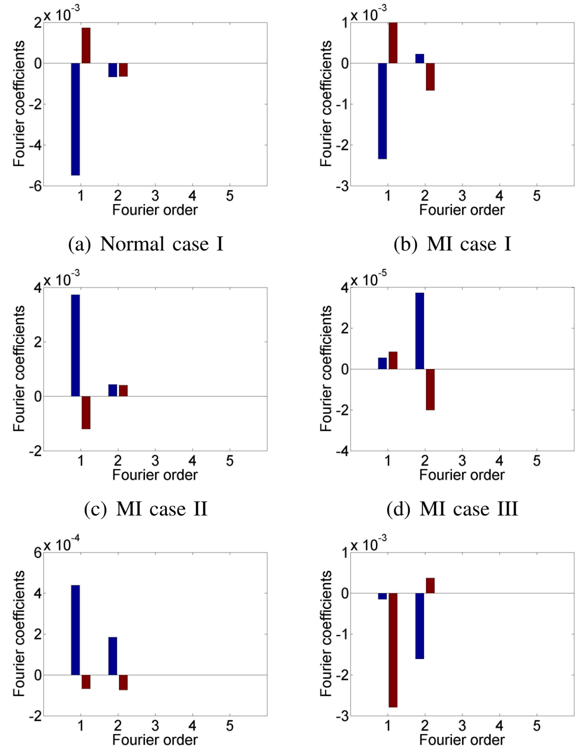


(a) Normal case I (b) MI case I (c) MI case II (d) MI case III (e) MI case IV (f) MI case V

Fig. 6. Fourier Series for normal and MI patients in Figure 5

The fitting step was a minimization procedure as follows:

$$(\mathbf{a}, \mathbf{b}, \omega) = \arg\min_{\mathbf{a},\mathbf{b},\omega} \sum_{t=t_1}^{t_{22}} |f((\mathbf{a}, \mathbf{b}, \omega, t) - C(t)|^2 . \quad (5)$$

The fitting step eliminated the high frequency component in the curvedness signal, which reflected the ventricular motion to some extent. The obtained parameters, i.e., the Fourier coefficients, and the Fourier Series represent the major components in the time-varying signal. From observation, we could detect some significant differences between the normal participants and the MI patients as shown in Figure 5.

### C. Feature Selection and Unsupervised Learning

Fourier coefficients, i.e., $\mathbf{a}, \mathbf{b}$, of all the 16 regions constitute the feature vector, $\mathbf{v}_i = \begin{bmatrix}\mathbf{a}\\ \mathbf{b}\end{bmatrix}$, see Figure 6. Two classic unsupervised learning (clustering) algorithms, i.e., k-means and fuzzy c-means, were applied on the data containing the mixed normal and patient features. The number of expected clusters was assigned.

## III. RESULTS

The study consists of nine normal cases and fifty-seven cases with myocardial infarction. The fifty-seven cases include thirty patients scanned at 3-6 months after MI and twenty-seven follow-up scanned at 9-12 months thereafter. All subjects were recruited without consideration of gender or ethnicity, and has given informed consent. The whole procedure was approved by the human subjects review committee of the National Heart Centre, Singapore.

All subjects were imaged on a 1.5T Siemens scanner. A parallel stack of two dimensional cine LV short-axis images were acquired via segmented k-space and retrospective electrocardiographic gating. The parallel short-axis imaging planes were located from the LV base to apex (8 mm interslice thickness with no interslice gap). The field of view was typically 320 mm with spatial resolution of less than 1.5 mm (typically 1.43 mm). Each slice was acquired in a single breath hold, with 22 temporal frames per cardiac cycle.

Second order Fourier series were used to fit the curvedness signal in each region of each subject. Four Fourier coefficients, i.e., $\mathbf{a}_1$, $\mathbf{a}_2$, $\mathbf{b}_1$,$\mathbf{b}_2$, were obtained for each region. The feature for each subject was a $1$ by $64$ vector. Both k-means and fuzzy c-means clustering algorithms were applied to the random ordered data. The clustering results from the two algorithms were identical. The accuracy (the ratio of the correctly clustered number to the total number) was $89\%$. The Rand Index was $0.8075$ and the adjusted Rand Index was $0.5374$. Hubert's index was $0.6149$ and Mirkin's index was $0.1925$. All the evaluation on the clustering result indicate a

TABLE I
TABLE OF CONFUSION

| | |
|---|---|
| 8 true negatives (AML 0.8599) | 1 false positives (AML 0.7226) |
| 6 false negatives (AML 0.7800) | 51 true positives (AML 0.9093) |

high similarity of the clustered result to the gold standard.

In the fuzzy c-means algorithm, a membership level was also assigned to each data entry, i.e., the confidence that this data belongs to which clusters. The average membership levels (AML) were computed for four groups in the table of confusion as well. From a diagnosis context, the false negative cases are usually fatal compared to the false positive cases. Our experiments show a lower false negative rate $0.1176$ than the false positive rate $0.1250$.

## IV. CONCLUSION

In this study, we proposed an approach to analyze the left ventricular dynamics in terms of curvedness value. The pipeline consisting of image processing, surface reconstruction, geometry analysis, and unsupervised learning, was successfully performed on 66 subjects. High clustering accuracy and other evaluation indices indicate the effectiveness of the curvedness value for assisting diagnosis. Future relevant work includes a more comprehensive analysis of the relation between the geometric dynamics and various medical conditions.

## ACKNOWLEDGMENT

This work was supported in part by SERC Biomedical Engineering Programme Grants 121 148 0003, 132 148 0012, Singhealth Foundation (SHF/FG408P/2009, SHF/FG453P/2011, SHF/FG503P/2012), NHCS Centre Grant Seed Funding (NHCS-CGSF/2014/003), Goh Cardiovascular Research Grant (Duke-NUS-GCR/2013/0009) and Singapore-China Joint Research Programme (1215c013). The financial support of Biomedical Research Council Research Grant (14/1/32/24/002) are gratefully acknowledged.

## REFERENCES

[1] Y. Nakayama, G. Shimizu, Y. Hirota, T. Saito, M. Kino, Y. Kitaura, and K. Kawamura, "Functional and histopathologic correlation in patients with dilated cardiomyopathy: an integrated evaluation by multivariate analysis," *Journal of the American College of Cardiology*, vol. 10, no. 1, pp. 186–192, 1987.

[2] J. N. Cohn, R. Ferrari, and N. Sharpe, "Cardiac remodelingconcepts and clinical implications: a consensus paper from an international forum on cardiac remodeling," *Journal of the American College of Cardiology*, vol. 35, no. 3, pp. 569–582, 2000.

[3] B. Swynghedauw, "Molecular mechanisms of myocardial remodeling," *Physiological reviews*, vol. 79, no. 1, pp. 215–262, 1999.

[4] W. Hayashida, T. Kumada, R. Nohara, H. Tanio, M. Kambayashi, N. Ishikawa, Y. Nakamura, Y. Himura, and C. Kawai, "Left ventricular regional wall stress in dilated cardiomyopathy." *Circulation*, vol. 82, no. 6, pp. 2075–2083, 1990.

[5] N. G. Bellenger, J. M. Francis, C. L. Davies, A. J. Coats, and D. J. Pennell, "Establishment and performance of a magnetic resonance cardiac function clinic," *Journal of Cardiovascular Magnetic Resonance*, vol. 2, no. 1, pp. 15–22, 2000.

[6] J. Lessick, S. Sideman, H. Azhari, E. Shapiro, J. Weiss, and R. Beyar, "Evaluation of regional load in acute ischemia by three-dimensional curvatures analysis of the left ventricle," *Annals of biomedical engineering*, vol. 21, no. 2, pp. 147–161, 1993.

[7] P. Germain, G. Roul, B. Kastler, J.-M. MOSSARD, P. Bareiss, and A. Sacrez, "Inter-study variability in left ventricular mass measurement comparison between m-mode echography and mri," *European heart journal*, vol. 13, no. 8, pp. 1011–1019, 1992.

[8] J. L. Gutiérrez-Chico, J. L. Zamorano, L. Pérez de Isla, M. Orejas, C. Almería, J. L. Rodrigo, J. Ferreirós, V. Serra, and C. Macaya, "Comparison of left ventricular volumes and ejection fractions measured by three-dimensional echocardiography versus by two-dimensional echocardiography and cardiac magnetic resonance in patients with various cardiomyopathies," *The American journal of cardiology*, vol. 95, no. 6, pp. 809–813, 2005.

[9] L. Zhong, D. N. Ghista, E. Y. Ng, S. T. Lim, T. S. Chua, and C. N. Lee, "Left ventricular shape-based contractility index," *Journal of biomechanics*, vol. 39, no. 13, pp. 2397–2409, 2006.

[10] R. Semelka, E. Tomei, S. Wagner, J. Mayo, C. Kondo, J. Suzuki, G. Caputo, and C. Higgins, "Normal left ventricular dimensions and function: interstudy reproducibility of measurements with cine mr imaging." *Radiology*, vol. 174, no. 3, pp. 763–768, 1990.

[11] J. F. DEBATIN, S. N. NADEL, H. D. SOSTMAN, C. E. SPRITZER, A. J. EVANS, and T. M. GRIST, "Magnetic resonance imaging-cardiac ejection fraction measurements: phantom study comparing four different methods," *Investigative radiology*, vol. 27, no. 3, pp. 198–203, 1992.

[12] P. Balzer, A. Furber, S. Delépine, F. Rouleau, F. Lethimonnier, O. Morel, A. Tadéi, P. Jallet, P. Geslin, and J.-J. le Jeune, "Regional assessment of wall curvature and wall stress in left ventricle with magnetic resonance imaging," *American Journal of Physiology-Heart and Circulatory Physiology*, vol. 277, no. 3, pp. H901–H910, 1999.

[13] M. Baroni, "Computer evaluation of left ventricular wall motion by means of shape-based tracking and symbolic description," *Medical engineering & physics*, vol. 21, no. 2, pp. 73–85, 1999.

[14] K. E. Leung and J. G. Bosch, "Localized shape variations for classifying wall motion in echocardiograms," in *Medical Image Computing and Computer-Assisted Intervention–MICCAI 2007*. Springer, 2007, pp. 52–59.

[15] L. Zhong, Y. Su, S.-Y. Yeo, R.-S. Tan, D. N. Ghista, and G. Kassab, "Left ventricular regional wall curvedness and wall stress in patients with ischemic dilated cardiomyopathy," *American Journal of Physiology-Heart and Circulatory Physiology*, vol. 296, no. 3, pp. H573–H584, 2009.

[16] M. Wan, Y. Wang, and D. Wang, "Variational surface reconstruction based on delaunay triangulation and graph cut," *International journal for numerical methods in engineering*, vol. 85, no. 2, pp. 206–229, 2011.

[17] M.-L. Tan, Y. Su, C.-W. Lim, S. K. Selvaraj, L. Zhong, and R.-S. Tan, "A geometrical approach for automatic shape restoration of the left ventricle," *PloS one*, vol. 8, no. 7, p. e68615, 2013.

[18] L. Zhong, L. Gobeawan, Y. Su, J.-L. Tan, D. Ghista, T. Chua, R.-S. Tan, and G. Kassab, "Right ventricular regional wall curvedness and area strain in patients with repaired tetralogy of fallot," *American Journal of Physiology-Heart and Circulatory Physiology*, vol. 302, no. 6, pp. H1306–H1316, 2012.

[19] J. Goldfeather and V. Interrante, "A novel cubic-order algorithm for approximating principal direction vectors," *ACM Transactions on Graphics (TOG)*, vol. 23, no. 1, pp. 45–63, 2004.

[20] C. Kambhamettu and D. B. Goldgof, "Curvature-based approach to point correspondence recovery in conformal nonrigid motion," *CVGIP: Image Understanding*, vol. 60, no. 1, pp. 26–43, 1994.

[21] L. Zhong, S. Y. Yeo, Y. Su, T. T. Le, R. San Tan, and D. Ghista, "Regional assessment of left ventricular surface shape from magnetic resonance imaging," in *Engineering in Medicine and Biology Society, 2007. EMBS 2007. 29th Annual International Conference of the IEEE*. IEEE, 2007, pp. 884–887.

[22] R. V. Garimella and B. K. Swartz, "Curvature estimation for unstructured triangulations of surfaces," *Los Alamos National Laboratory*, 2003.

[23] F. Cazals and M. Pouget, "Estimating differential quantities using polynomial fitting of osculating jets," *Computer Aided Geometric Design*, vol. 22, no. 2, pp. 121–146, 2005.

[24] J. J. Koenderink and A. J. van Doorn, "Surface shape and curvature scales," *Image and vision computing*, vol. 10, no. 8, pp. 557–564, 1992.

[25] L. Zhong, R.-S. Tan, D. N. Ghista, E. Y.-K. Ng, L.-P. Chua, and G. S. Kassab, "Validation of a novel noninvasive cardiac index of left ventricular contractility in patients," *American Journal of Physiology-Heart and Circulatory Physiology*, vol. 292, no. 6, pp. H2764–H2772, 2007.